Journal of Statistical Physics, Vol. 36, Nos. 5/6, 1984

Multiparticle Fractal Aggregation

Richard F. Voss[1]

Kinetic fractal aggregation in a particle bath where a fraction f of the sites are initially occupied is studied with $d = 2$ computer simulations. Independent particles diffusing to a fixed cluster produce an aggregate with fractal dimension $D \simeq 1.7$ up to a correlation length $\xi(f)$. At larger lengths $D \to 2$. $\xi(f) \to \infty$ as $f \to 0$. When the particles remain fixed but the cluster undergoes a rigid random walk D appears constant at larger scales but varies with f. $D \to 1.95$ at large f and $D \to 1.7$ as $f \to 0$. In both cases, the aggregate size $N(t)$ grows with time t as $t^{\gamma(f)}$. Aggregation on a surface by independently diffusing particles produces shapes reminiscent of electrochemical dendritic growth. The dependence of growth rate and geometry is studied as a function of particle concentration and sticking probability.

KEY WORDS: Aggregation; fractal; dendritic growth; diffusion.

Many growth or aggregation phenomenon result in fractal clusters[1,2] with power law correlations over wide ranges of length scales. Such correlations are reminiscent of those found in equilibrium phase transitions at the critical point. Much of the recent widespread interest in understanding the origins of these correlations is based on the success of computer simulations[3–5] in reproducing the scale-invariant properties. In particular, a simple model has been presented[3,4] for the aggregation process when the limiting step is diffusion to the growth sites. This model is based only on local constraints (Brownian motion, connectivity to aggregate) yet it reproduces the long-range fractal behavior. This model and its variations have also stimulated theoretical treatments based on mean field[6] and continuum[7–9] approximations and real space renormalization.[10]

The models presented here are a generalization of the single-particle diffusion-limited aggregation process.[3] In that model, a single particle

[1] IBM Thomas J. Watson Research Center, Yorktown Heights, New York 10598.

0022-4715/84/0900-0861$03.50/0 © 1984 Plenum Publishing Corporation

would undergo a random walk until reaching the boundary of the aggregate or cluster. At this point it became part of the cluster and a new particle began its walk. The result for $d = 2$ was a ramified cluster with a two-point density correlation function that varies as $1/r^{\eta}$ with $\eta \simeq 0.3$. Such aggregates are most conveniently characterized within the framework of Mandelbrot's fractal geometry[2] by their fractal dimension $D = d - \eta$. In this case, the radius of gyration R is also related to N, the number of particles in the cluster, by $N \propto R^D$.

In this paper, the specific effect of multiple particles on the resulting aggregate geometry is studied with $d = 2$ computer simulations. This modification results in a model more closely resembling actual growth situations and, moreover, enables a study of the growth rate vs. concentration. For both of the variations presented, aggregate growth occurs in a particle bath where a fraction f of the sites are initially occupied. The particles are mutually exclusive and only one particle can occupy a given site during each time step.

The first variation consists of initially populating a fraction f of the available sites on a two-dimensional square lattice with mobile particles and starting a cluster "seed" at the origin. During a time step, each of the mobile particles is examined in random order. One of its neighbor sites is selected by chance as a possible next position. If unoccupied, the particle moves to this new site. If occupied, the particle remains fixed. If the new site borders the cluster, the particle and any of its neighbors also become part of the cluster. The simulation boundaries are held fixed at the initial concentration f and the process is iterated while the cluster growth is recorded.

Samples of the cluster grown by this multiparticle diffusive aggregation (MPDA) and its particle bath are shown in Fig. 1. Cluster sites are shown as solid black squares while the mobile particles are the surrounding smaller dots. Figure 1a shows a MPDA cluster of 5000 atoms grown in a concentration $f = 0.05$. A depletion layer with few mobile particles is clearly seen outside the cluster boundary. This cluster is extremely similar to those produced by the single-particle process.[3,4] Figure 1b, shows a MPDA cluster of 10000 atoms grown in a higher concentration $f = 0.25$. In this case, the cluster is much more compact and the surrounding depletion layer is very narrow. In these higher concentrations cluster growth is extremely rapid and in Fig. 1b it is possible to see several mobile particles "trapped" within the growing cluster that have not yet become attached.

The second variation also begins by occupying a fraction f of the available sites and positioning a cluster "seed" at the origin. In this case, however, the particles remain fixed while the growing cluster undergoes a random walk. At each time step, the cluster moves rigidly and without rotation by one lattice site in a random direction. Any particles neighboring

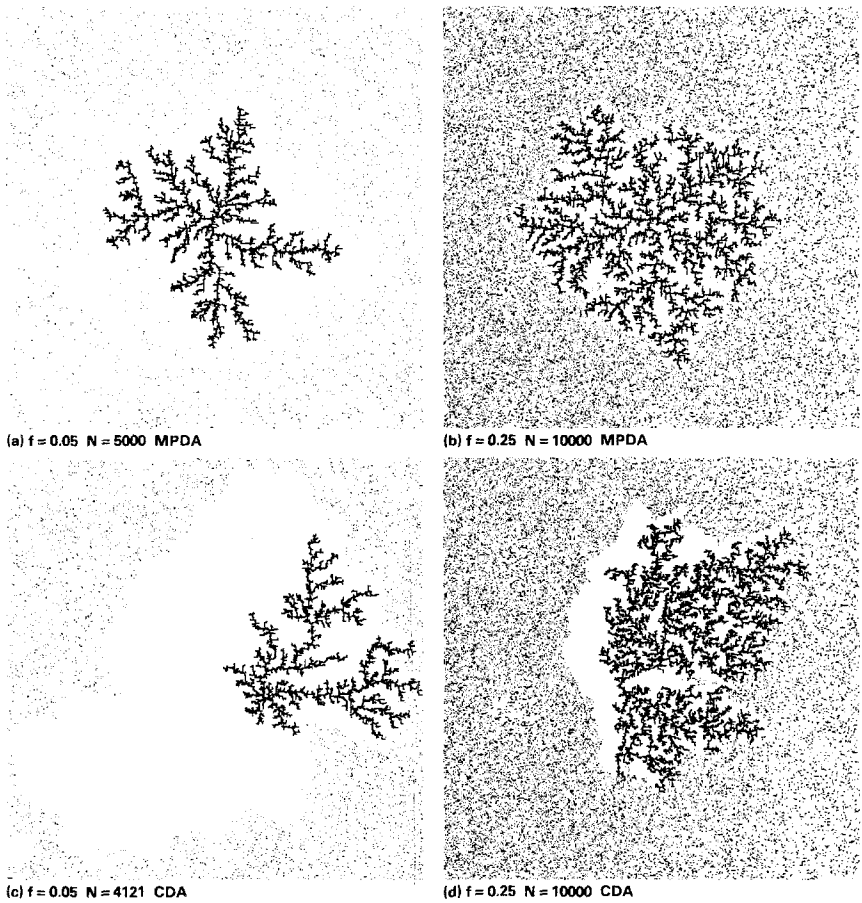

Fig. 1. Samples of multiparticle diffusive aggregates. (a) and (b) simultaneous diffusion of particles in concentration f to fixed aggregate. (c) and (d) cluster diffusion through fixed particles of concentration f.

the cluster become attached. As the cluster moves, it grows by consuming its environment. Growth stops when the cluster reaches the edge of the initial lattice.

Samples of the result of this cluster diffusion aggregation (CDA) are also shown in Fig. 1. Figure 1c shows a CDA cluster of 4121 atoms grown in a concentration $f = 0.05$. The depleted area swept out by the cluster random walk is clearly seen. This cluster is also similar to those produced by the single-particle process.[3,4] Figure 1d, shows a CDA cluster of 10000 atoms grown in a higher concentration $f = 0.25$. As with Fig. 1b the cluster is more compact at higher f. Differences are, however, visible. The MPDA

clusters in Fig. 1a and 1b are relatively symmetric about their origin, while the CDA clusters of Fig. 1b and 1d show much more variation at large scales.

Multiple clusters have been simulated using both the MPDA and CDA processes at various f in the range 0.02 to 0.50 and with typical sizes N from 20000 to 450000 atoms. As with percolation,[11,12] all of these clusters are ramified with a perimeter/area ratio that is a constant at large N. This ratio increases slightly as f increases. Although radius of gyration $R(N)$ variations with N have been used to estimate the fractal dimension D for the clusters, the geometric differences at various f are most clearly seen in the two-point density correlation function $g(R)$. Effectively $R(N)$ averages the contributions only about the center of mass while $g(R)$ averages over all points in the cluster. Here, $g(R)$ is the probability that two points separated by a distance R are both part of the aggregate. Fractal, or scale-invariant, shapes are characterized by power law $g(R) \propto 1/R^{\eta}$ up to length scales of order of the cluster radius. Two-dimensional fast Fourier transform (FFT) routines were used to estimate the two-dimensional spectral density of the aggregates and then to determine $g(R)$.

Figure 2 shows $g(R)$ vs. R for six large clusters grown by multiple particles at different f diffusing to a fixed seed (MPDA). In all cases the rapid decrease in $g(R)$ at $R \simeq 200$ is due the finite cluster size. At low concentrations, $f < 0.08$, the $g(R)$ for different f are indistinguishable and follow the simple power law indicated by the straight line $g(R) \propto 1/R^{\eta}$ with $\eta \simeq 0.28$ in Fig. 2. This η corresponds to a fractal dimension $D = 2 - \eta \simeq 1.7$ in agreement with previous single-particle aggregation simulations[3,4] and $R(N)$ variations. This correspondence is expected. At low f only one particle is effectively in the cluster neighborhood at one time. As the concentration f is increased, $g(R)$ follows the low-f limit at low R, then becomes approximately constant before falling off at the cluster radius. Thus, at larger f the aggregate properties are fractal or scaling only out to some effective correlation length $\xi(f)$. For length scales λ such that $\xi(f) < \lambda < R$ the aggregate properties are roughly uniform with $D \to 2$. This transition is visible in Fig. 1b where the aggregate has a relatively uniform appearance over intermediate length scales.

The inset in Fig. 2 shows $\xi(f)$ as a function of f estimated from the $g(R)$ transition from power law to constant. As f increases $\xi(f) \to 0$ while at low f $\xi(f) \to \infty$. The $\xi(f)$ dependence shown is consistent with a functional dependence $\xi(f) \propto 1/f^2$ or $\xi(f) \propto \exp[-f^{1/2}]$. The data are, however, insufficient to distinguish between these two forms or other possibilities. Theoretical treatments that include a finite particle density also suggest the introduction of a new length corresponding to the maximum size for fractal behavior. A mean-field[6] approximation introduces a diffusion screening

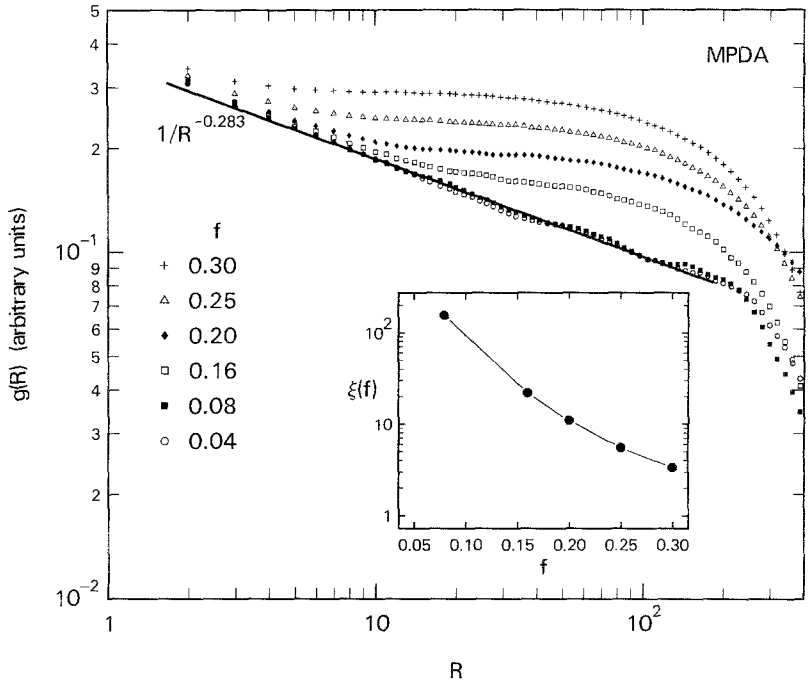

Fig. 2. Two-point correlation function $g(R)$ vs. R for multiple particles at different concentrations f diffusing to a fixed cluster. Solid line shows limiting $1/R^{\eta}$ behavior at low f. Inset shows how correlation length ξ varies with f.

length varying as f^{-1}, while a continuum approach[9] suggests a boundary layer varying as $1/f^{\theta}$ with $\theta \simeq 1$ as a new critical exponent.

Figure 3 shows the measured $g(R)$ for cluster diffusion through fixed particles (CDA) at various f. Although there is some indication of an effective $\xi(f)$ similar to Fig. 2 with $\xi(f) \to \infty$ as $f \to 0$, the clusters do not become uniform on length scales $>\xi(f)$. For $R > \xi$, the observed $g(R)$ follows a power law for all R up to the cluster radius. The solid lines in Fig. 3 show fits to the form $g(R) \propto 1/R^{\eta}$ and the resulting η are tabulated. Once again, at low f the results are (as expected) consistent with the single particle simulations where $D = 2 - \eta \simeq 1.7$. In this case, however, the aggregates apparently remain fractal at larger scales up to their radius, while D appears to vary continuously with f. This surprising fractal (as opposed to uniform) behavior is visible by comparing Fig. 1d with 1b. There is no scale at which the overall appearance of Fig. 1d becomes uniform. These CDA simulations were performed with much larger clusters than the MPDA results in Fig. 2 to study the apparent variable D at larger R. Figure 3 appears to be inconsistent with an interpretation of a slow crossover at all f

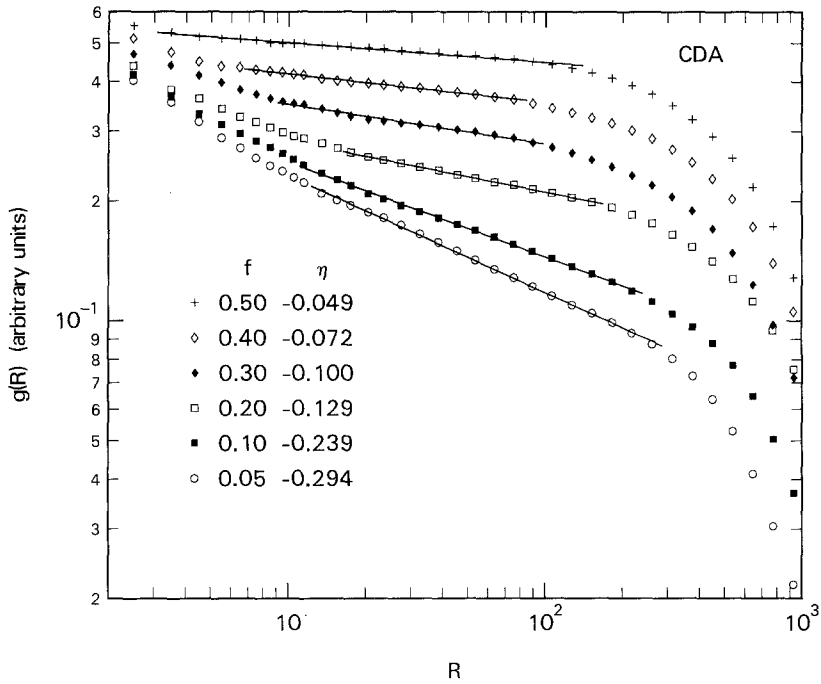

Fig. 3. Two-point correlation function $g(R)$ vs. R for rigid cluster diffusing through different concentrations f of fixed particles. Solid lines show fits to $g(R) \propto 1/R^{\eta}$.

to uniform behavior. The theoretical models[6–9] that predict such behavior do not apply to the CDA process, and even larger simulations would be necessary to ascertain if the apparent D persists as $R \to \infty$. The fact that growth occurs in a concentration f does not necessarily constrain the aggregate large-R behavior to approach $D = 2$. A model where the only allowed growth sites are the two opposite ends of a rod would always produce a linear aggregate with $D = 1$ in any f. Moreover, CDA, like all aggregation models, is a nonequilibrium time-varying process. The fractal dimension D characterizes a "snapshot" of the system at one instant in time. As shown in Fig. 1, at large f, an aggregate grows rapidly and $g(R)$, which represents only those particles that are part of the aggregate, can decrease below f because of the voids "inside" the aggregate that still contain unattached particles. At a later time, the particles in these voids will have joined the aggregate, but other, larger voids will have appeared.

At large f, these CDA aggregates seem to have a limiting $D \simeq 1.95$ and it is interesting to speculate on the connection with percolation.[11,12] For $f \to p_c$, the percolation threshold ($p_c \simeq 0.59$ for four-neighbor connectivity

on a square lattice) the points connected to the original "seed" have a large extent even before the seed moves. Thus, as $f \to p_c$ the initial configuration becomes a large "seed" having the fractal dimension of the "infinite" percolation cluster[12] $D_{pc} \simeq 1.9$ and η_{pc} (for a single cluster) $\simeq 0.1$. Once the "seed" begins to move it rapidly sweeps up the remaining (initially unattached) particles and $D \to 1.95$ while $\eta \simeq \eta_{pc}/2 \simeq 0.05$.

One of the advantages of these multiparticle simulations is the possibility of getting information about the growth of the aggregate in time. Figure 4a shows the measured aggregate growth $N(t)$ vs. time t for MPDA at

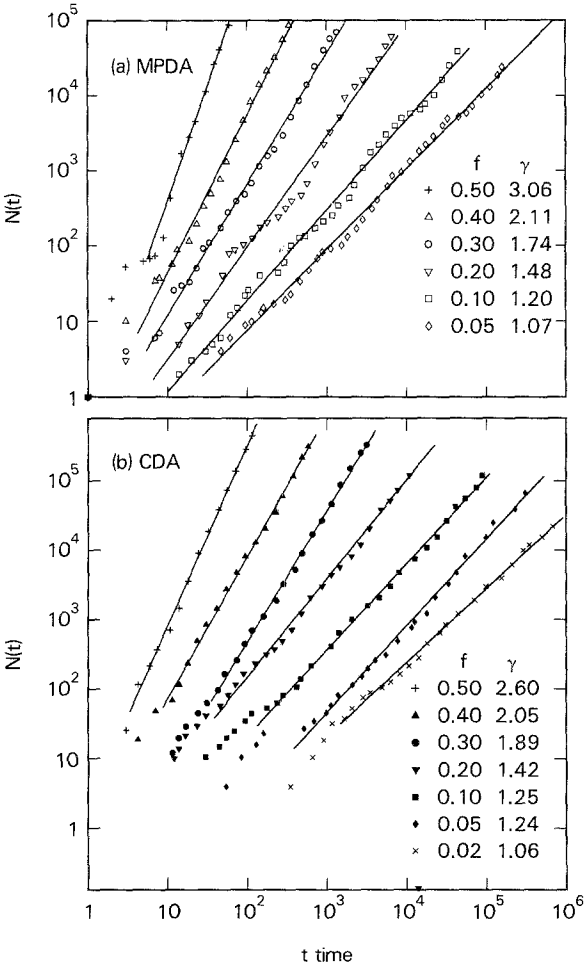

Fig. 4. Time dependence of cluster size $N(t)$ for MPDA (a) and CDA (b) aggregates grown in different concentrations f. Solid lines show fits to $N(t) \propto t^{\gamma(f)}$.

various f. Unit time corresponds to the possible movement of each of the mobile bath particles by one site. Figure 4b shows the same quantity for the cluster diffusion aggregation (CDA) where the cluster undergoes one displacement in each time step. For both processes, the observed aggregate size $N(t)$ is best described as a power law t^{γ} where γ is a function of f. In both cases $\gamma(f) \to 1$ as $f \to 0$ while $\gamma(f)$ increases rapidly as $f \to p_c$ the percolation threshold. For $d \geqslant 3$, a spherically symmetric analytical model[13] predicts power law $N(t)$ with an exponent that varies with d but not with f. Extension of this result[13] to two-dimensions predicts $\gamma = 1$ with logarithmic corrections. Although the large f simulations in Fig. 4 were carried out to sizes many orders of magnitude larger than $\xi(f)$, there is no indication of a crossover to a behavior independent of f.

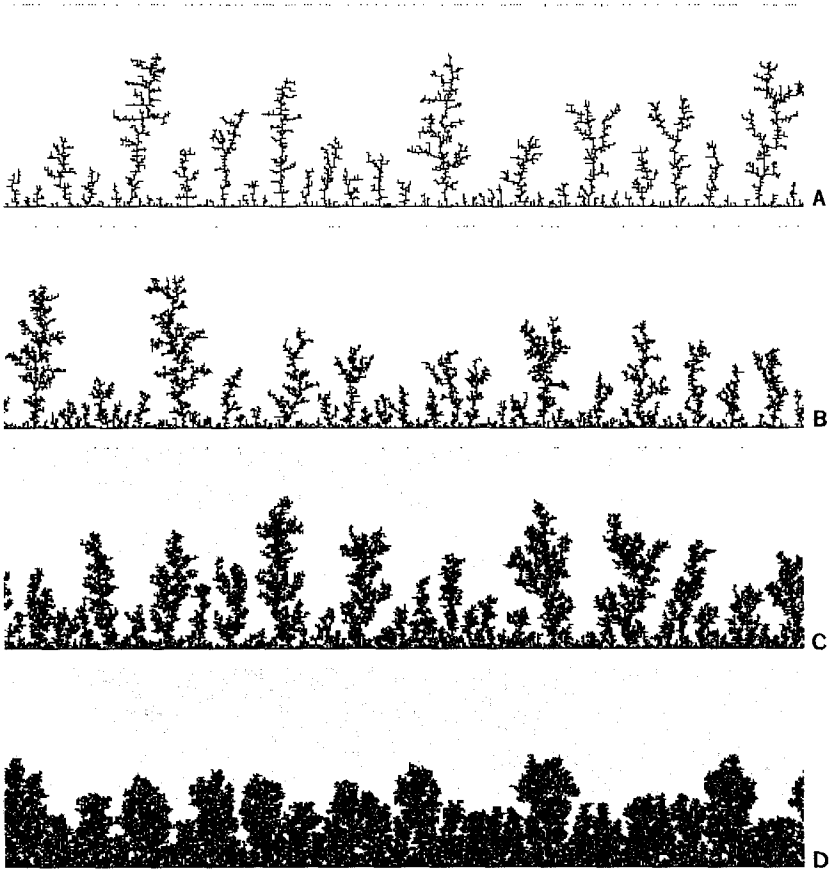

Fig. 5. MPDA aggregate growth on a surface from a concentration $f = 0.05$. (a) sticking probability, $s = 1.0$; (b) $s = 0.2$; (c) $s = 0.05$; (d) $s = 0.01$.

There are, of course, many other variations of the fractal aggregation process. For example, the effect of varying the sticking probability s has been investigated for single-particle aggregation.[3] It was found that $s < 1$ introduces small-scale correlation. In addition, the obvious similarity of these fractal aggregates to actual dendrites suggests a study of growth from a surface (as opposed to an initial point as discussed above). For the specific case of electrochemical dendrites,[14] experiments typically study the growth rate of dendrite height for differing ionic solution concentrations and current density. The measurements themselves are somewhat subjective both in differentiating between "dendritic growth" and "rough surfaces" and in determining a procedure for measuring dendritic height. There is an obvious correspondence between the electrolytic solution concentration and the

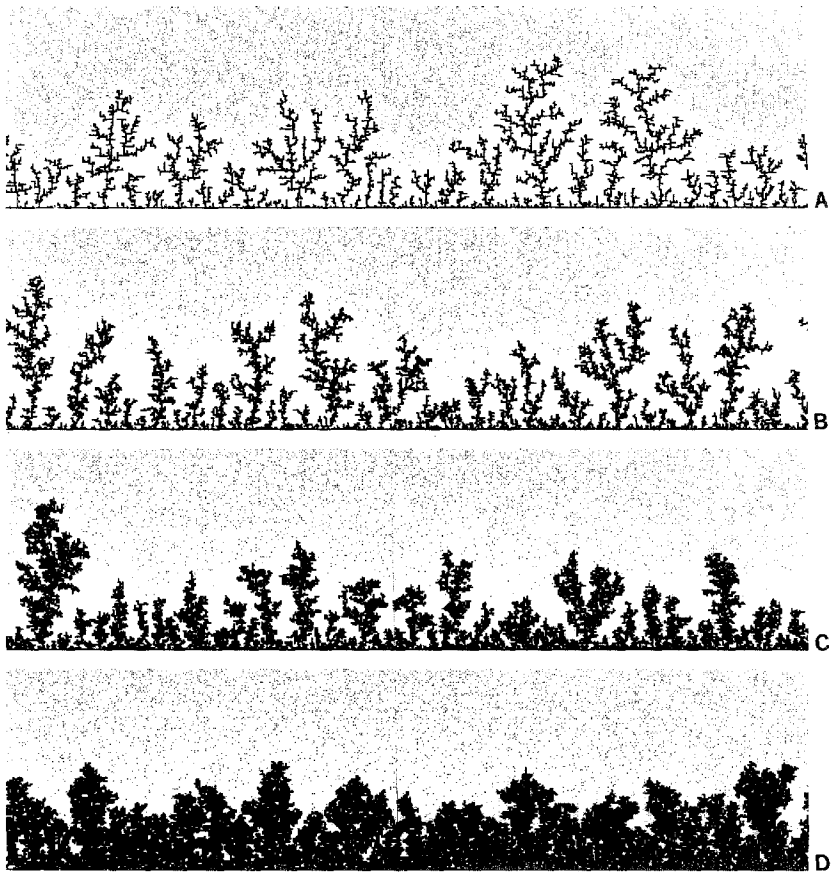

Fig. 6. MPDA aggregate growth on a surface from a concentration $f = 0.20$. (a) sticking probability, $s = 1.0$; (b) $s = 0.2$; (c) $s = 0.05$; (d) $s = 0.01$.

simulation particle density f. Similarly, one expects the ionic current density to be related to the sticking probability s: as the current density or $s \to 0$ there is no net attachment of particles to the surface. Figures 5–7 show samples of MPDA aggregation onto a horizontal surface for different varying f and s. The top of each sample was held at the initial concentration f while the aggregate grew from the bottom up. Periodic boundary conditions were used in the horizontal direction. Figures 5–7 demonstrate that many of the qualitative features of electrolytic deposition (from "rough surface" to "dendrites") are readily found with the two-dimensional MPDA simulations by varying only f and s.

The simulations provide a straightforward estimate of average surface height vs. time over many more orders of magnitude than the typical

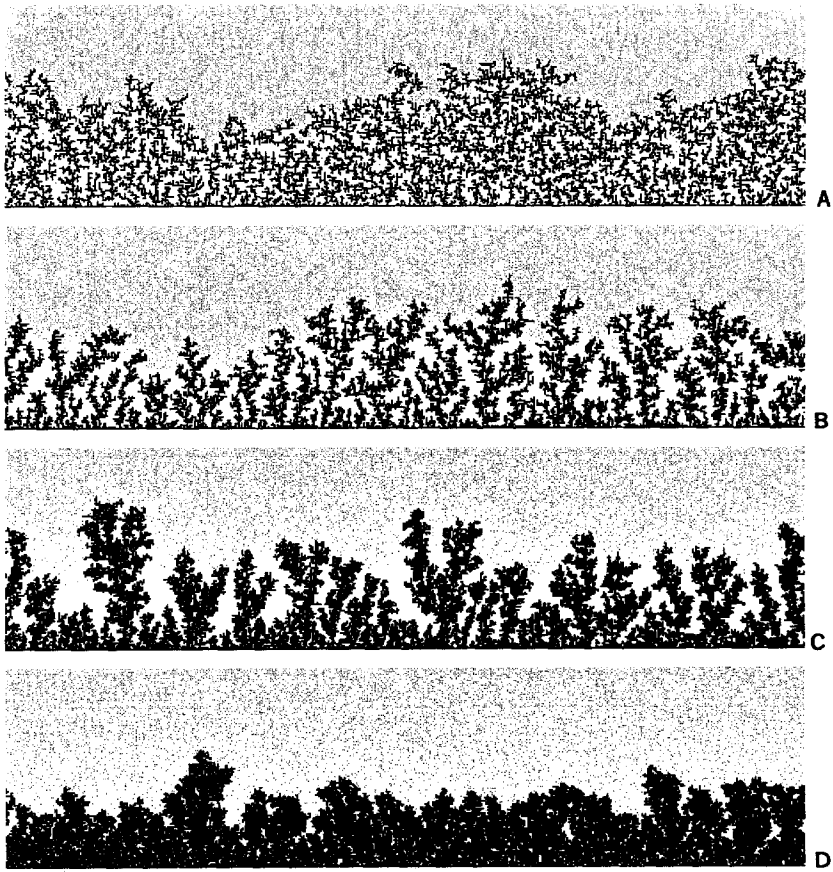

Fig. 7. MPDA aggregate growth on a surface from a concentration $f = 0.40$. (a) sticking probability, $s = 1.0$; (b) $s = 0.2$; (c) $s = 0.05$; (d) $s = 0.01$.

experiment. Figure 8 shows average surface height vs. time for simulations with differing f and s. For a wide variety of (but not all) conditions the average surface height varies approximately as $t^{2/3}$. A detailed comparison of these two-dimensional simulations with actual three-dimensional electrolytic growth experiments is underway.[15]

In summary, new multiparticle models of kinetic fractal aggregation have been studied with $d = 2$ computer simulations. Independent particles of initial concentration f diffusing to a fixed cluster produce an aggregate with fractal dimension $D \simeq 1.7$ up to a correlation length $\xi(f)$. At larger lengths

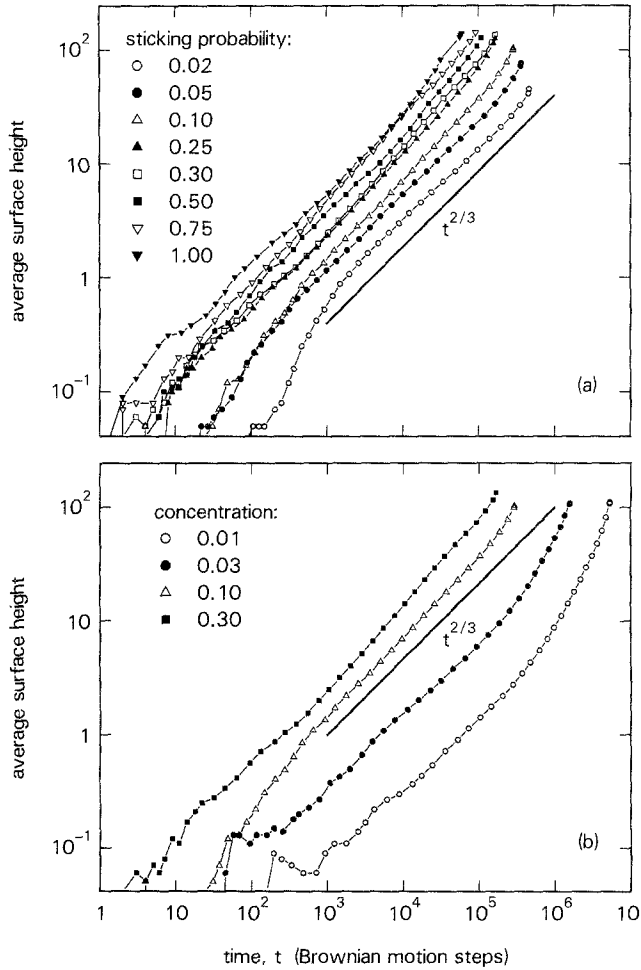

Fig. 8. Time dependence of the average aggregate height vs. time for (a) growth in a concentration $f = 0.10$ at various sticking probabilities, s; and (b) growth with $s = 0.10$ at various f.

the cluster becomes uniform and $D \to 2$. $\xi(f) \to \infty$ as $f \to 0$. For a cluster undergoing rigid Brownian motion through fixed particles the aggregate appears to have a variable fractal dimension $D(f)$ at larger scales. $D \to 1.95$ at large f and $D \to 1.7$ as $f \to 0$. For both models, the aggregate growth is described as $N(t) \propto t^{\gamma(f)}$ at large t. $\gamma(f) \to 1$ as $f \to 0$. Aggregation on a surface by independently diffusing particles produces shapes reminiscent of electrochemical dendritic growth. Changes in particle density f and sticking probability s simulate observed electrochemical variations in solution concentration and current density. The average rate dependence on f and s is studied.

ACKNOWLEDGMENTS

Helpful discussions with B. B. Mandelbrot and Micha Tomkiewicz are gratefully acknowledged.

REFERENCES

1. S. R. Forrest and T. A. Witten, *J. Phys. A* **12**:L109 (1979).
2. B. B. Mandelbrot, *The Fractal Geometry of Nature* (Freeman, New York, 1982).
3. T. A. Witten and L. M. Sander, *Phys. Rev. Lett.* **47**:1400 (1981); *Phys. Rev. B* **27**:5686 (1983).
4. P. Meakin, *Phys. Rev. A* **27**:604 (1983).
5. R. F. Voss, *Bull. Am. Phys. Soc.* **28**:487 (1983); *Phys. Rev. B* **30**:334 (1984).
6. M. Muthukumar, *Phys. Rev. Lett.* **50**:839 (1983).
7. R. Ball, M. Nauenberg, and T. Witten, NSF ITP preprint.
8. M. Nauenberg, *Phys. Rev. B* **28**:449 (1983).
9. M. Nauenberg, R. Richter, and L. M. Sander, *Phys. Rev. B* **28**:449 (1983).
10. H. Gould, F. Family, and H. E. Stanley, *Phys. Rev. Lett.* **50**:686 (1983).
11. D. Stauffer, *Phys. Rep.* **54**:1 (1979).
12. R. F. Voss, R. B. Laibowitz, and E. I. Alesandrini *Phys. Rev. Lett.* **49**:1441 (1982).
13. J. M. Deutch and P. Meakin, *J. Chem. Phys.* **78**:2093 (1983).
14. J. O'M. Bockris and G. A. Razumney, *Fundamental Aspects of Electrocrystallization* (Plenum Press, New York, 1967).
15. M. Tomkiewicz and R. F. Voss, to be published.